# Magnetic states of *M*-Fe wires (*M*=Sc–Ni) on vicinal Cu(111) from first principles

H. Hashemi,[1,*] W. Hergert,[1] and V. S. Stepanyuk[2]
[1]*Institut für Physik, Martin-Luther-Universität Halle-Wittenberg, Von-Seckendorff-Platz 1, D-06120 Halle, Germany*
[2]*Max-Planck-Institut für Mikrostrukturphysik, Weinberg 2, D-06120 Halle, Germany*
(Received 23 March 2009; revised manuscript received 29 December 2009; published 24 March 2010)

One-dimensional transition-metal (TM) nanowires of single atom width can be formed on a stepped Cu(111) surface, as pointed out by Mo *et al.* [Phys. Rev. Lett. **94**, 155503 (2005)] for Fe on Cu(111). The basic template is an embedded Fe chain at one-atom distance away from the upper edge of the monatomic surface step. Chains, consisting of 3*d* TM atoms from Sc to Ni can be formed on top of the Fe chain. Density-functional theory is applied to calculate the magnetic ground state and to describe the magnetic properties of such TM-Fe wires. The wires form different magnetic structures but are all characterized by a high local magnetic moment.

DOI: 10.1103/PhysRevB.81.104418 PACS number(s): 75.75.−c, 73.63.Nm, 75.70.−i

## I. INTRODUCTION

The development of high-density magnetic recording devices is one driving force to investigate new nanostructured magnetic materials. Among others one-dimensional (1D) periodic linear arrangements of atoms (chains) have been investigated from experimental[1–5] and theoretical points of view.[6–16] Most of the experimental methods and, in a much stronger sense, possible applications need a high packing density of such chains.

A stepped surface is a common template to create one-dimensional nanostructures.[17] The main idea is to exploit the 1D symmetry provided by an array of parallel steps on a vicinal surface. Along this surface, the deposited material can nucleate a procedure called step decoration. Chains or nanostripes usually grow on lower terraces along an ascending step edge. Cu surfaces can be prepared with lots of atom-high steps. Surprisingly, the observations of Shen *et al.*[1,2] have demonstrated that Fe nanostripes grow on the upper terrace of a stepped Cu(111) surface.

An important investigation to elucidate the growth of linear Fe nanostructures on a stepped Cu(111) surface was made by Mo *et al.*[16] The investigation of elementary diffusion and exchange processes of Fe atoms on a stepped Cu(111) surface by means of *ab initio* calculations based on density-functional theory (DFT) proved the existence of a special kinetic pathway of the formation of Fe nanowires on stepped Cu(111) surfaces. Kinetically the growth of linear Fe nanostructures is a two-stage process. At first, Fe adatoms form an atom chain embedded into the Cu substrate behind a row of Cu atoms at the descending step [cf. Figs. 1(a) and 1(b)]. This formation of a linear 1D Fe structure makes the row of embedded Fe atoms very stable. In a following step, the embedded Fe chain acts as an attractor for the Fe atoms deposited on the surface. Therefore, a secondary chain of Fe atoms is formed on top of the embedded Fe chain [cf. Fig. 1(c)] since Fe-Fe bonds are stronger than Fe-Cu bonds. As a result, a very stable atom-wide iron nanowire is formed on the Cu surface, one chain is buried in the surface behind a step and the second chain on top of the first. Total-energy calculations revealed that the position of the Fe chain at the upper edge is energetically favorable to a Fe chain located at the step edge but only under the condition that another row of Fe atoms is incorporated underneath the exposed row.[16]

Subsequently to Ref. 16, in a scanning tunneling microscopy investigation aided by DFT calculations, Guo *et al.*[3] have confirmed the growth process. A careful study of all atomic processes in the line of Ref. 16 has been used to perform kinetic Monte Carlo calculations.[18] The simulations demonstrate the growth process as predicted by Mo *et al.* and proved experimentally.[3]

Furthermore, the Cu(111) stepped surface with the embedded Fe chain can be considered as an exemplary template for the deposition of other 3*d* TM atoms to form a chain on top of the embedded Fe chain. It is the interplay between dimensionality, local environment, and magnetic properties which causes the special interest in such systems. For a clear notation, a single linear periodic arrangement of atoms will be called a chain in the following investigation while a system consisting of two parallel chains, either isolated or embedded in the Cu(111) surface, will be named wire.

TM chains have been considered in previous density-functional studies in different environments. Spišák and Hafner investigated metal chains at the step edge of vicinal Cu surfaces.[12–15] Infinite metal chains on flat surfaces have been studied in Ref. 10 while Ataca *et al.*[9] and Tung and Guo[8] focused on isolated chains. Finite chains on flat Cu and Ni surfaces have been considered in Refs. 6 and 7. Antiferromagnetic order has been found experimentally by Hirjibehedin *et al.*[4] for linear finite Mn chains created by atom manipulation on an insulating CuN/Cu(001) surface.

The present investigation provides a systematic discussion of one-dimensional magnetic nanostructures grown on a vicinal Cu(111) surface using the above-mentioned template [cf. Fig. 1(b)]. Our study is focused on 3*d* transition metals from Sc to Ni because they offer a wide scope of complex magnetic structures in higher dimensions and contain the bulk ferromagnets. In contrast to the previous theoretical investigations, we concentrate on the magnetic properties of mixed TM-Fe wires behind the step.

The paper is organized as follows. In Sec. II, the details of the performed *ab initio* calculations are given. The presentation of the results and the discussion in Sec. III starts with an explanation of the magnetic structures. Those structures are investigated for TM-Fe wires embedded in the Cu surface

 

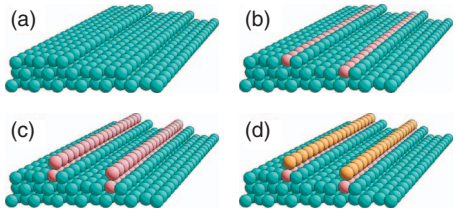


FIG. 1. (Color) Growth of TM-Fe double chains on Cu(111): (a) clean Cu(111) stepped surface. (b) Deposition of Fe atoms (brown) on a stepped Cu (blue) surface. The Fe chain is embedded in the step behind a row of Cu atoms. (c) One-atom-wide Fe nanowire (brown) is formed, one chain of Fe embedded in the surface behind the step, the second Fe chain is formed on top of the first. (d) One-atom-wide TM nanowire (yellow) is formed on top of the embedded Fe chain.

and for comparison for isolated free-standing wires as well. A detailed compilation of the real structure data of the embedded TM-Fe wires follows. The ground-state energies and magnetic moments will be discussed in detail. Special emphasis is placed on the properties of Cr-Fe and Mn-Fe wires.

## II. COMPUTATIONAL DETAILS

The calculations have been performed within the framework of spin-polarized density-functional theory, using the Vienna *ab initio* simulation package (VASP).[19,20] The frozen-core full-potential projector-augmented-wave method is used,[21] applying the generalized gradient approximation of Perdew and Wang.[22] The default cutoff energies of the plane-wave basis sets, depending on the transition-metal elements, are applied. The Methfessel-Paxton scheme[23] is employed for Brillouin-zone integrations. Structural relaxations have been performed using the quasi-Newton algorithm, and stopped when the forces acting on all the unconstrained ions have dropped below 0.01 eV/Å. During structural relaxations, the bottom three layers of the six-layer slab are fixed at their ideal bulk positions (calculations using an eight-layer slab lead to insignificant changes in energy differences between the magnetic configurations). The convergence of the calculated properties with respect to the number of $k$ points and supercell size was carefully checked. The bulk lattice constant of fcc Cu was estimated to be $a=3.633$ Å. This is in good agreement with the experimental value of $a=3.615$ Å at room temperature[24] and $a=3.603$ Å, the value extrapolated to $T=0$ K.[25] The isolated chains and wires have been modeled as a two-dimensional array of infinitely long units, keeping the distance to be at least 13 Å. 12 $k$ points are used to sample half of the one-dimensional Brillouin zone. A supercell containing six Cu layers, which corresponds to 60 Cu atoms, was constructed to model the Cu(111) stepped surface. The Cu slab was rotated in turn by a slab miscut along the (322) direction. Therefore, at the end, the system consists of (111) terraces separated by {100}-faceted steps of monatomic height. The same construction was used by Mo *et al.*[16] The terraces are five lattice constants wide. The distance from one slab to its nearest image was equivalent to 13.5 Å. In all calculations, the two-dimensional Brillouin zone was sampled using a $20\times5$ mesh. The template constructed in this way is shown in Fig. 1(a).

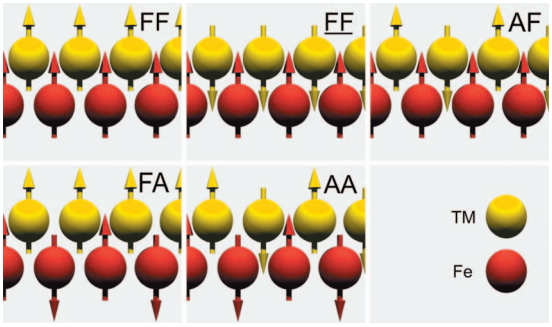


FIG. 2. (Color) Schematic view of the five magnetic configurations considered for nanowires consisting of TM (yellow) and Fe (red) chain. FF: ferromagnetic structure, FF: ferromagnetic chains are coupled antiferromagnetically, AF: the antiferromagnetic TM chain is coupled to the ferromagnetic Fe chain, FA: the ferromagnetic TM chain couples to the antiferromagnetic Fe chain, and AA: antiferromagnetic arrangement.

## III. RESULTS AND DISCUSSION

### A. Magnetic structures

If a nanowire consisting of a TM and a Fe chain (TM-Fe wire) is constructed, a series of different magnetic structures is possible. We will restrict our investigation to four atoms per unit cell. In this case, five different magnetic structures can be formed. All the structures are depicted schematically in Fig. 2. The notation of the magnetic structures throughout the paper is such that the first letter (A—antiferromagnetic and F—ferromagnetic) characterizes the TM chain while the second letter characterizes the embedded Fe chain. To distinguish the two possible directions of moments if both chains are ferromagnetically ordered, an antiferromagnetic coupling between the chains is marked by an underscore FF. Three structures result from a ferromagnetically ordered Fe chain (FF, FF, AF). In principal, also the Fe chain could order antiferromagnetically. Two additional magnetic structures can be formed. Either the TM chain exhibits ferromagnetic (FA) or antiferromagnetic order (AA). The calculations reveal that configurations with antiferromagnetic order (FA, AA) of the embedded Fe chain are energetically not favorable. Such structures are not taken into account in the following discussion.

### B. Real structure of embedded TM-Fe wires

Information about structural relaxations are given in Tables I and II. Relaxations of the first three layers at the surface are considered. All relaxations are given for the magnetic ground-state configuration. The relaxations are given in percentages of the ideal values, i.e., in-plane relaxations ($\Delta y$) are expressed in terms of the ideal Cu bond length $d_{\mathrm{Cu}}=2.569$ Å whereas the interlayer relaxations are calculated with respect to the ideal interlayer distance of $d_{12}=2.098$ Å.

TABLE I. Lateral and vertical relaxations of the clean Cu(111) vicinal surface, the Cu(111) surface with the embedded Fe chain, and the Cu(111) surface with the embedded Fe-Fe wire. Relaxations are given with respect to the ideal lattice positions. Lateral relaxations are expressed as percentage of the ideal bond length 2.569 Å. Vertical relaxations along the (111) direction are given as percentages of the interlayer distance 2.098 Å. The relaxations are presented for the surface (s) and two subsurface layers and all rows of atoms (1)–(5) parallel to the step in the terrace. The shifts $\Delta y$ and $\Delta z$ correspond to differences between relaxed and ideal structure, i.e., $\Delta z$ is positive for an outward relaxation perpendicular to the surface.

| | Vicinal Cu(111) | | | | | | | | | |
|---|---|---|---|---|---|---|---|---|---|---|
| | Row | | | | | | | | | |
| | (1) | | (2) | | (3) | | (4) | | (5) | |
| Layer | $\Delta y$ | $\Delta z$ | $\Delta y$ | $\Delta z$ | $\Delta y$ | $\Delta z$ | $\Delta y$ | $\Delta z$ | $\Delta y$ | $\Delta z$ |
| (s) | 2.4 | 2.7 | 1.2 | −0.9 | 0.2 | −1.1 | −1.2 | −0.5 | −3.8 | −4.4 |
| (s-1) | 0.2 | 0.5 | −0.4 | 0.6 | 0.0 | −0.3 | 0.3 | −0.4 | 1.7 | −1.0 |
| (s-2) | −0.1 | 0.2 | −0.1 | 0.4 | −0.3 | 0.3 | −0.3 | 0.0 | 0.0 | 0.3 |
| | Fe chain embedded in Cu(111) | | | | | | | | | |
| (s) | 1.4 | 3.1 | −0.3 | 0.2 | −1.4 | 0.3 | −2.8 (Fe) | −0.9 (Fe) | −5.2 | −2.6 |
| (s-1) | 0.2 | 0.6 | 0.1 | 1.1 | 0.2 | 0.2 | 0.4 | −0.8 | 1.2 | −0.7 |
| (s-2) | 0.2 | 0.1 | 0.2 | 0.6 | −0.1 | 0.5 | −0.2 | −0.3 | 0.2 | −0.1 |
| | Embedded Fe chain of Fe-Fe wire in Cu(111) | | | | | | | | | |
| (s) | 1.1 | 5.2 | −0.2 | 1.8 | −1.0 | 5.3 | −2.7 (Fe) | −5.9 (Fe) | −6.4 | −0.7 |
| (s-1) | 1.2 | 1.2 | 0.5 | 2.5 | 1.1 | 3.1 | −0.4 | −4.1 | 1.5 | −1.2 |
| (s-2) | 0.6 | 0.2 | 0.8 | 1.2 | 0.3 | 2.0 | −0.6 | −1.5 | 0.9 | −0.9 |

The relaxations of the clean Cu(111) surface are compared with relaxations in presence of an embedded Fe chain and a Fe-Fe wire [cf. Figs. 1(c) and 1(d)]. The nomenclature used in the table is explained in the schematic view given in Fig. 3. The relaxations in the second subsurface layer (s-2) are small, in general. The relaxations in (s-1) are larger but only significant at the step edge. The relaxations of the surface layer of Cu(111) are dominated by two effects. The lateral relaxation are pointed to the center of the terrace causing a compression. The lateral relaxation $\Delta y$ at site (3) in the middle of the terrace is small. In general, the surface layer shows an inward relaxation. At the step edge, site (5), the inward relaxation is large. Together with the outward relaxation at site (1), the relaxations reduce the interatomic distances at the step edge.

The relaxations change significantly if one row of Cu atoms is substituted by one row of Fe behind the step edge. From structural point of view, a decrease in the inward relaxations is obtained associated with increased lateral relaxations. Therefore, the tendency of a terrace compression is increased by the embedded Fe chain. If the Fe-Fe wire is formed, the embedded Fe chain experiences a strong inward relaxation. Although the lateral relaxations are nearly unchanged within the terrace, the outward relaxation of the Cu atoms is strongly enhanced. Due to structural changes connected with the formation of TM-Fe wires, changes in the

TABLE II. Relative relaxations of the TM-Fe wires deposited on the surface. The ground-state MS is also indicated.

| | | TM | | Fe | |
|---|---|---|---|---|---|
| TM | MS | $\Delta y$ | $\Delta z$ | $\Delta y$ | $\Delta z$ |
| Sc | FF | −4.7 | −19.8 | −0.8 | −2.1 |
| Ti | FF | −5.0 | −28.5 | 0.6 | −0.2 |
| V | FF | −6.3 | −33.2 | 1.8 | 0.1 |
| Cr | AF | −0.5(−3.8) | −4.4(−24.2) | −4.0 | −6.2 |
| Mn | FF | −3.0 | −15.8 | −4.2 | −6.4 |
| Fe | FF | −3.1 | −22.5 | −2.7 | −5.9 |
| Co | FF | −4.8 | −25.8 | −2.3 | −6.1 |
| Ni | FF | −4.6 | −23.9 | −5.0 | −8.7 |

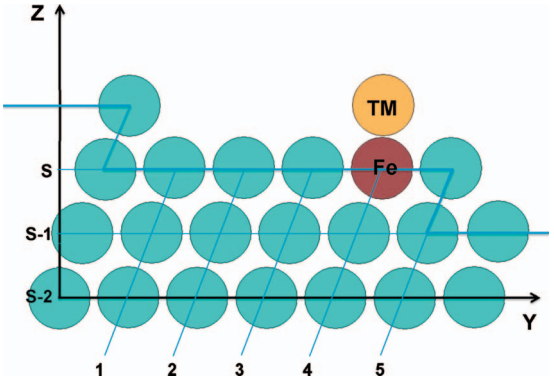


FIG. 3. (Color) Schematic view of the stepped surface. The nomenclature of the figure is used in Tables I and II. The shifts $\Delta y$ and $\Delta z$ correspond to differences between relaxed and ideal structure, i.e., $\Delta z$ is positive for an outward relaxation perpendicular to the surface.

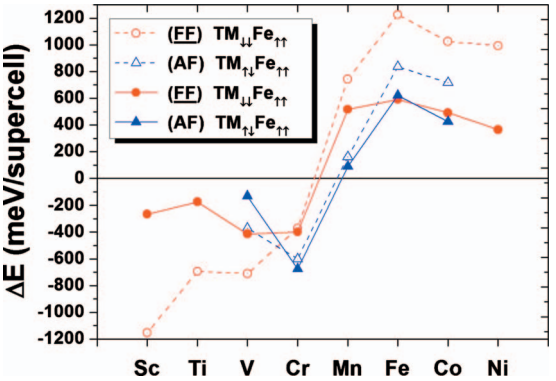


FIG. 4. (Color) Total energy of the FF and the AF states relative to the FF magnetic structure. The solid symbols are related to the embedded wires and the open symbols stand for the isolated TM-Fe wire. The energy calculations for the embedded structures are based on the relaxed structures.

magnetic properties can be expected if compared to calculations based on ideal structures.[26]

The relaxations after forming a TM-Fe wire [cf. Fig. 1(d)] are summarized in Table II. The relaxations at sites (1–3) and (5) in the surface do not change significantly compared to the situation of an embedded Fe-Fe wire, therefore Table II contains relaxations of the TM and the Fe chains only. The magnetic ground state of the corresponding system is also indicated in the table. Three magnetic ground states are obtained (cf. Fig. 2). The antiferromagnetic (AF) structure of Cr leads to special effects in the real structure. Therefore, Cr will be discussed separately. The TM chains having FF and FF magnetic structures show an inward relaxation toward the Fe chain and a shift away from the step. $\Delta y$ and $\Delta z$ have the same order of magnitude for all those systems. The antiferromagnetic coupling of the ferromagnetic TM chain (Sc-V) reduces the inward relaxation of the Fe chain significantly. The TM-Fe wires formed by late TM (Mn-Ni) couple ferromagnetically (FF). The relaxation of the embedded Fe chain is nearly unchanged as it can be deduced from Table II.

The detailed investigation of real structure effects of FF and FF structures proofs the strong correlation between magnetic and real structure in those quasi-one-dimensional systems. Therefore, especially the Cr-Fe wire, having an AF magnetic ground-state structure, should show an interesting relaxation pattern. It should be noted that magnetic frustration will lead, in general, to a noncollinear magnetic structure (MS) for this wire, which will reduce the relaxations compared to the strictly collinear calculations of the present paper. The Cr-Fe wire minimizes the energy by adopting a zigzag-like structure in the plane perpendicular to the surface. The inward relaxations are 4.4% and 24.2% for Cr($\uparrow,\downarrow$). Also the lateral relaxations show a zigzag structure of 0.5% and 3.8% for Cr($\uparrow,\downarrow$) away from the step. The relaxations of the Cr atoms are connected with an inward relaxation of −6.2% of the embedded Fe chain and 7% of dimerization. The dimerization which is observed only for AF structures may be interpreted as a result of repulsive (attractive) nature of the magnetic contribution to the interaction energy of Cr (Fe) pairs in Cu.[27]

### C. Electronic and magnetic ground-state properties

#### *1. Magnetic ground-state structure*

The relative stability of the different magnetic structures is the most interesting question in our investigation. The data are summarized in Fig. 4. The energy differences $\Delta E$ (in millielectron volt per supercell) are defined relative to the FF structure. Energy differences larger than zero indicate a stable FF structure while $\Delta E<0$ denotes the stability of FF or AF structure. The magnetic structures of the embedded wires are calculated in fully relaxed geometries.

The bulk ferromagnets Fe, Co, and Ni lead to a ferromagnetic TM-Fe wire in this low-dimensional configuration. If we assume an ideal structure for Mn (nonrelaxed), a bistability between FF and AF magnetic structures ($\Delta E\approx 13$ meV/supercell) is observed.[26] This bistability is lifted including relaxations and the energy difference becomes considerably larger, stabilizing the FF structure. [$\Delta E\approx 89$ meV/supercell, cf. Fig. 4]. It was not possible to stabilize AF structures in our calculations for Sc, Ti, and Ni. The Cr-Fe wire shows an AF structure.

Energy differences for the isolated TM-Fe wires are given in Fig. 4 for comparison. The isolated wire is calculated in an ideal linear structure corresponding to the Cu bond length $d_{\mathrm{Cu}}$. The embedding of the wires has a large effect on the FF magnetic structure of all the $3d$ TM but $\Delta E$ changes only marginal for most of the calculated AF structures. The comparison of magnetic structures of unrelaxed isolated wires with the embedded wires shows that the magnetic structures practically do not change. The most interesting system of the $3d$ series investigated here is the Cr-Fe wire. It is characterized by large local Cr($\uparrow,\downarrow$) moments of $3.4\mu_B$ and $3.3\mu_B$. Both, FF and AF structures are practically not influenced by the embedding in the Cu surface. The AF structure is the ground state. It was pointed out by Mo *et al.*[3] that the adatom position on the embedded Fe chain represents a local energy minimum, independent of the type of the atom. From this point of view, the formation of structurally well-ordered antiferromagnetic Cr chains on top of the Fe template chain should be experimentally feasible.

The magnetic properties of the ground-state configurations will be discussed in more detail. The magnetic properties of isolated TM chains and TM-Fe wires will be used as a reference in the discussion. The ideal bond length $d_{Cu}$ in accordance with the Cu bulk lattice constant is assumed for the calculation of those idealized structures. Although isolated TM chains show effects such as dimerization and formation of a zigzag structure (cf. Refs. 8 and 9), we do not allow such effects to have well-defined reference structures.

The total energies of possible magnetic structures have been calculated to find the ground state. The calculations reveal that the ground states of the TM chains, TM-Fe wires, and the embedded structures are the same for most of the systems. Exceptions appear for Sc, V, and Mn. While the free Sc chain is nonmagnetic, the Sc-Fe wire exhibits the FF structure in the isolated and the embedded case. The isolated V chain shows ferromagnetic coupling while the isolated V-Fe wire and the corresponding embedded system exhibit an FF structure. The isolated Cr and Mn chains are antiferromagnetically coupled. The coupling to Fe in the isolated Mn-Fe wire accounts for the FF structure being the ground state of embedded Mn-Fe as well.

Our calculations can be compared with results for fully relaxed linear chains by Tung and Guo.[8] The equilibrium bond lengths in the relaxed chains are up to 20% smaller than the Cu bond length assumed in our calculations. Only Sc shows a 10% larger bond length. The equilibrium magnetic structures in the relaxed geometry given in Ref. 8 are nevertheless the same as in our artificial structure strained to the Cu bond length, with V as an exception. It is not surprising that the V chain is ferromagnetic at the Cu bond length because its relaxed interatomic distance is only 1.2% different from $d_{Cu}$ in the ferromagnetic state, in contrast to a 20.2% smaller one with respect to the Cu bond length in the antiferromagnetic state. Fixing the bond length to $d_{Cu}$ leads to the suppression of the Sc magnetic moment. Starting from a linear chain and fixing the distance of next-nearest neighbors to $2d_{Cu}$, a relaxation of the AF Cr chain leads to a zigzag deformation with an angle of 153°. This angle is 160° if the chain is deposited on top of the embedded Fe chain.

### *2. Magnetic moments*

The magnetic moments of the ground states of all systems are given in Fig. 5. In general, the magnetic moments of the TM atoms in the TM-Fe wire are smaller than in the isolated TM chain. However, Sc is polarized and obtains a sizable moment, the Cr moment decreases and the Mn moment is practically unchanged. The Fe moment in the different wire systems is nearly constant and larger than the bulk value. Note that our calculated magnetic moments for bulk ferromagnetic metals Fe, Co, and Ni are 2.23 $\mu_B$/atom, 1.65 $\mu_B$/atom, and 0.67$\mu_B$/atom, respectively. The combination of a TM chain with the Fe chain is connected with an increase in the coordination number of the atoms. This leads, in general, to a decrease in the moments. Due to the embedding, each TM atom will beside the two Fe neighbors, get two additional Cu atoms as nearest neighbors. The moment of the template Fe chain is reduced by about 0.5$\mu_B$. The TM moments are only slightly reduced. Our investigation reveals

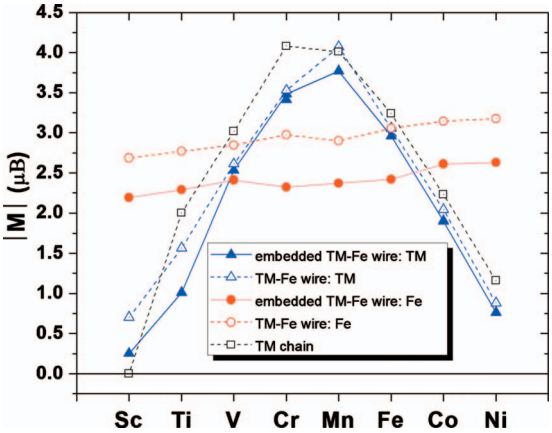


FIG. 5. (Color) Absolute magnetic moments of the ground-state configurations. (a) isolated TM chain and isolated TM-Fe wire. An ideal structure based on the Cu lattice constant is assumed. (b) TM-Fe wire embedded in Cu(111) surface. The structure is relaxed.

that from the 3$d$ series, Cr-Fe and Mn-Fe wires are the most promising systems for experimental investigations. In all configurations considered here, Cr shows an antiferromagnetic coupling. Embedding has practically no effect on the stability of the AF structure. The latter is very stable with respect to the other magnetic structures. The bistability detected for the Mn-Fe system in the nonrelaxed structure was the starting point to investigate if changes in the lattice constant could force the Mn-Fe wire to switch to the AF structure. Stress or strain perpendicular to the wire does not change the magnetic structure. 5% stress in direction of the wire leads to an AF ground state. Let us assume that the physics of the formation of the template Fe chain will not change if an appropriate substrate, i.e., a few Cu layers with a stepped (111) surface deposited on an adequate substrate which causes the strain in the Cu film, leads to a stress of some percent in direction of the Mn-Fe wire. In this case, one could speculate that a switching of the magnetic state by external means might be possible.

## IV. CONCLUSIONS

In summary, we have performed first-principles calculations of magnetic states in TM-Fe wires on the vicinal Cu surface. The Fe chain near the step of the Cu(111) surface is the template for the formation of TM chains in atop position of the Fe chain.

Ferromagnetic (Mn, Fe, Co, and Ni) as well as antiferromagnetic structures (Cr) might be achieved using the embedded Fe wire near the step as a template. The antiferromagnetic structure of Cr is very robust. Therefore, the formation of long antiferromagnetic Cr chains on top of the Fe template chain should be experimentally feasible. Stress could be used to prepare Mn-Fe wires in ferromagnetic or antiferromagnetic structure. The systematic investigation of different

magnetic states, as presented in this paper can be used as a starting point to consider the finite-temperature magnetic properties of such TM-Fe wires. If the energy differences of the different magnetic states are mapped on a classical Heisenberg model, the nearest-neighbor exchange parameters $J_{\text{TM-TM}}, J_{\text{Fe-Fe}}, J_{\text{TM-Fe}}$ can be determined. Subsequent Monte Carlo calculations can be used to determine the magnetic properties at finite temperature.

## ACKNOWLEDGMENTS

We thank N. N. Negulyaev and P. A. Ignatiev for fruitful discussions. The work was supported by the cluster of excellence "Nanostructured Materials" of the state Saxony-Anhalt and the International Max Planck Research School for Science and Technology of Nanostructures.

*hossein.hashemi@physik.uni-halle.de

[1] J. Shen, R. Skomski, M. Klaua, H. Jenniches, S. S. Manoharan, and J. Kirschner, Phys. Rev. B **56**, 2340 (1997).
[2] J. Shen, M. Klaua, P. Ohresser, H. Jenniches, J. Barthel, C. V. Mohan, and J. Kirschner, Phys. Rev. B **56**, 11134 (1997).
[3] J. Guo, Y. Mo, E. Kaxiras, Z. Zhang, and H. H. Weitering, Phys. Rev. B **73**, 193405 (2006).
[4] C. F. Hirjibehedin, C. P. Lutz, and A. J. Heinrich, Science **312**, 1021 (2006).
[5] P. Gambardella, A. Dallmeyer, K. Maiti, M. C. Malagoli, W. Eberhardt, K. Kern, and C. Carbone, Nature (London) **416**, 301 (2002).
[6] S. Lounis, P. H. Dederichs, and S. Blügel, Phys. Rev. Lett. **101**, 107204 (2008).
[7] B. Lazarovits, L. Szunyogh, P. Weinberger, and B. Újfalussy, Phys. Rev. B **68**, 024433 (2003).
[8] J. C. Tung and G. Y. Guo, Phys. Rev. B **76**, 094413 (2007).
[9] C. Ataca, S. Cahangirov, E. Durgun, Y.-R. Jang, and S. Ciraci, Phys. Rev. B **77**, 214413 (2008).
[10] Y. Mokrousov, G. Bihlmayer, S. Blügel, and S. Heinze, Phys. Rev. B **75**, 104413 (2007).
[11] Y. Mo, W. Zhu, E. Kaxiras, and Z. Zhang, Phys. Rev. Lett. **101**, 216101 (2008).
[12] D. Spišák and J. Hafner, Phys. Rev. B **65**, 235405 (2002).
[13] D. Spišák and J. Hafner, Phys. Rev. B **67**, 214416 (2003).
[14] D. Spišák and J. Hafner, Comput. Mater. Sci. **27**, 138 (2003).
[15] D. Spišák and J. Hafner, Comput. Mater. Sci. **30**, 278 (2004).
[16] Y. Mo, K. Varga, E. Kaxiras, and Z. Zhang, Phys. Rev. Lett. **94**, 155503 (2005).
[17] C. Tegenkamp, J. Phys.: Condens. Matter **21**, 013002 (2009).
[18] N. N. Negulyaev, V. S. Stepanyuk, W. Hergert, P. Bruno, and J. Kirschner, Phys. Rev. B **77**, 085430 (2008).
[19] G. Kresse and J. Hafner, Phys. Rev. B **48**, 13115 (1993).
[20] G. Kresse and J. Furthmüller, Phys. Rev. B **54**, 11169 (1996).
[21] P. E. Blöchl, Phys. Rev. B **50**, 17953 (1994).
[22] J. P. Perdew and Y. Wang, Phys. Rev. B **45**, 13244 (1992).
[23] M. Methfessel and A. T. Paxton, Phys. Rev. B **40**, 3616 (1989).
[24] M. E. Straumanis and L. S. Yu, Acta Crystallogr., Sect. A: Cryst. Phys., Diffr., Theor. Gen. Crystallogr. **25**, 676 (1969).
[25] A. K. Giri and G. B. Mitra, J. Phys. D **18**, L75 (1985).
[26] H. Hashemi, W. Hergert, and V. S. Stepanyuk, J. Magn. Magn. Mater. **322**, 1296 (2010).
[27] T. Hoshino, W. Schweika, R. Zeller, and P. H. Dederichs, Phys. Rev. B **47**, 5106 (1993).